



# Lepton angular distribution of $Z$ boson production and jet discrimination

Jen-Chieh Peng<sup>a,\*</sup>, Wen-Chen Chang<sup>b</sup>, Randall Evan McClellan<sup>c,a</sup>, Oleg Teryaev<sup>d</sup>

<sup>a</sup> Department of Physics, University of Illinois at Urbana–Champaign, Urbana, IL 61801, USA

<sup>b</sup> Institute of Physics, Academia Sinica, Taipei 11529, Taiwan

<sup>c</sup> Thomas Jefferson National Accelerator Facility, Newport News, VA 23606, USA

<sup>d</sup> Bogoliubov Laboratory of Theoretical Physics, JINR, 141980 Dubna, Russia

## ARTICLE INFO

### Article history:

Received 21 July 2019

Accepted 23 August 2019

Available online 27 August 2019

Editor: W. Haxton

### Keywords:

$Z$ -boson production

$Z$  decay angular distribution

jet discrimination

## ABSTRACT

High precision data of lepton angular distributions in inclusive  $Z$  boson production, reported by the CMS and ATLAS Collaborations, showed pronounced transverse momentum ( $q_T$ ) dependencies of the  $A_0$  and  $A_2$  coefficients. Violation of the Lam-Tung relation,  $A_0 = A_2$ , was also found. An intuitive understanding of these results can be obtained from a geometric approach. We predict that  $A_0$  and  $A_2$  for  $Z$  plus single gluon-jet events are very different from that of  $Z$  plus single quark-jet events, allowing a new experimental tool for checking various algorithms which attempt to discriminate quark jets from gluon jets. We also predict that the Lam-Tung relation would be more severely violated for the  $Z$  plus multiple-jet data than what has been observed so far for inclusive  $Z$  production data. These predictions can be readily tested using existing LHC data.

© 2019 The Authors. Published by Elsevier B.V. This is an open access article under the CC BY license (<http://creativecommons.org/licenses/by/4.0/>). Funded by SCOAP<sup>3</sup>.

Measurement of lepton angular distribution in  $W$  and  $Z$  boson production has long been advocated as a sensitive tool for understanding the production mechanism of these gauge bosons [1,2]. The lepton angular distribution in  $Z$  boson production was first measured by the CDF Collaboration for  $\bar{p}p$  collision at 1.8 TeV [3]. More recently, the CMS [4] and ATLAS [5] Collaborations at LHC reported high-statistics measurements of the lepton angular distribution of  $Z$  boson production in  $pp$  collision at  $\sqrt{s} = 8$  TeV. Pronounced  $q_T$  dependencies, where  $q_T$  refers to the transverse momentum of  $Z$  boson, were observed for the lepton angular distributions. The Lam-Tung relation [6], which is the analog of the Callan-Gross relation [7] in deep-inelastic scattering, was found to be significantly violated [4,5].

In a recent analysis [8,9] of the LHC  $Z$  boson angular distribution data, we showed that the  $q_T$  dependence of lepton angular distributions can be well described by an intuitive geometric approach. These data were shown to be sensitive to the relative contributions between the  $q\bar{q}$  annihilation and the  $qg$  Compton process. The violation of the Lam-Tung relation was attributed [8] to the acoplanarity between the ‘hadron plane’ and the ‘quark plane’,

to be defined later. The magnitude of the violation of the Lam-Tung relation was shown to depend on the amount of the acoplanarity.

The angular distribution data presented by the CMS and ATLAS Collaborations correspond to inclusive  $Z$  boson production. For  $Z$  boson produced with a sizable  $q_T$  there must be accompanying single jet or multiple jets to balance the  $q_T$  of the  $Z$ -boson. In this paper we show that new insight on the  $q_T$  dependence of the angular distribution coefficients, as well as the violation of the Lam-Tung violation, could be obtained if the angular distribution coefficients were analyzed as a function of the number of accompanying jets. We also show that the angular distribution coefficients for  $Z$  plus single jet data would provide a powerful tool for testing various algorithms designed to distinguish quark jets from gluon jets.

The lepton angular distribution in the  $Z$  rest frame can be expressed as [4,5]

$$\begin{aligned} \frac{d\sigma}{d\Omega} \propto & (1 + \cos^2 \theta) + \frac{A_0}{2} (1 - 3 \cos^2 \theta) + A_1 \sin 2\theta \cos \phi \\ & + \frac{A_2}{2} \sin^2 \theta \cos 2\phi + A_3 \sin \theta \cos \phi + A_4 \cos \theta \\ & + A_5 \sin^2 \theta \sin 2\phi + A_6 \sin 2\theta \sin \phi \\ & + A_7 \sin \theta \sin \phi, \end{aligned} \quad (1)$$

\* Corresponding author.

E-mail address: [jcpeng@illinois.edu](mailto:jcpeng@illinois.edu) (J.-C. Peng).

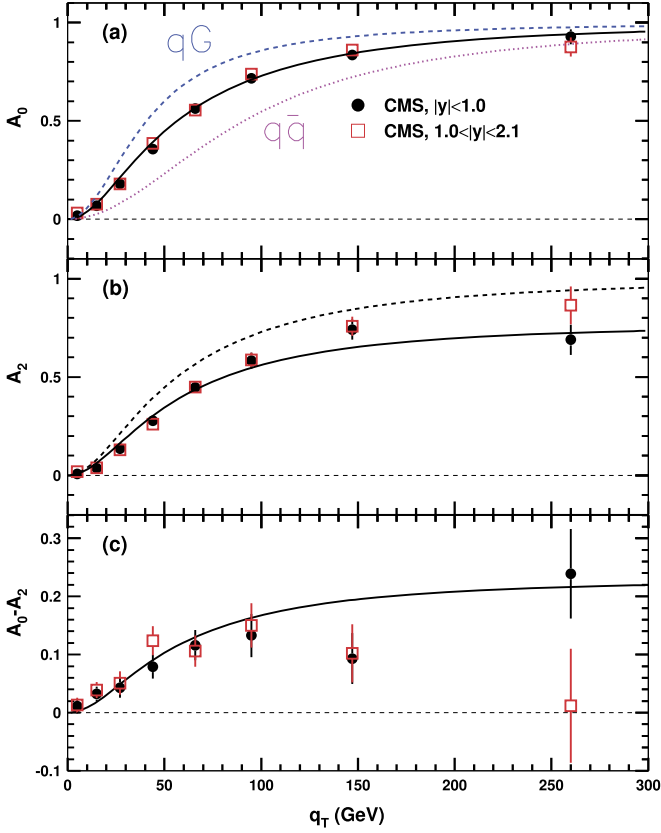


**Fig. 1.** The CMS data on  $A_0$ ,  $A_2$  and  $A_0 - A_2$  measured at two rapidity ( $y$ ) regions. The solid curves correspond to calculations based on the geometric model discussed in the text. The dotted and dashed curves in (a) are calculations for the  $q\bar{q}$  and  $qg$  processes, respectively. The dashed curve in (b) corresponds to the Lam-Tung relation,  $A_0 = A_2$ , where  $A_0$  is taken from the solid curve in (a).

where  $\theta$  and  $\phi$  are the polar and azimuthal angles of  $l^-$  ( $e^-$  or  $\mu^-$ ) in the rest frame of  $Z$ . The original Drell-Yan model [10] neglected QCD effects and intrinsic transverse momenta of the annihilating quark and antiquark. Hence, the angular distribution is simply  $1 + \cos^2\theta$  and all angular distribution coefficients,  $A_i$ , vanish. For non-zero dilepton transverse momentum,  $q_T$ , these coefficients can deviate from zero. However, it was predicted that the coefficients  $A_0$  and  $A_2$  should remain identical,  $A_0 = A_2$ , which is the Lam-Tung relation [6]. The high-statistics  $Z$  boson production data from the LHC allow a precise test of the Lam-Tung relation. Fig. 1 shows the CMS data for  $A_0$ ,  $A_2$ , and  $A_0 - A_2$  measured at two rapidity ( $y$ ) regions. Pronounced  $q_T$  dependence of  $A_0$  and  $A_2$  is observed. Moreover, the Lam-Tung relation,  $A_0 - A_2 = 0$ , is found to be clearly violated.

To provide some insight on the meaning of various angular distribution coefficients  $A_i$  in Eq. (1), we first present a derivation for Eq. (1) based on an intuitive geometric picture [8,9]. In the frame where  $Z$  is at rest, we define three different planes, namely, the hadron plane, the quark plane, and the lepton plane, shown in Fig. 2. For non-zero  $q_T$ , the momenta of the colliding hadrons,  $\vec{P}_B$  and  $\vec{P}_T$ , are no longer collinear and they form the “hadron plane” shown in Fig. 2. Various coordinate systems have been considered in the literature, and the Collins-Soper (C-S) frame [11] was used by both the CMS and ATLAS Collaborations. For the C-S frame, both the  $\hat{x}$  and  $\hat{z}$  axes lie in the hadron plane, and the  $\hat{z}$  axis bisects  $\vec{P}_B$  and  $-\vec{P}_T$  with an angle  $\beta$ . It is straightforward to show that

$$\tan \beta = q_T / Q, \quad (2)$$

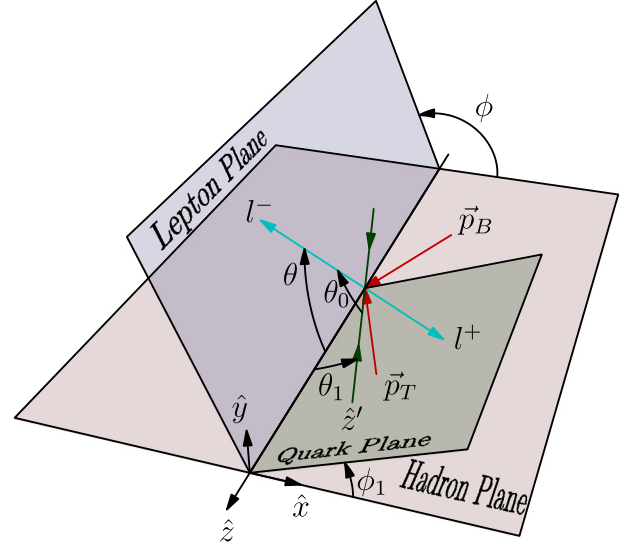


**Fig. 2.** Definition of the Collins-Soper (C-S) frame and various angles and planes in the rest frame of  $Z$  boson. The hadron plane is formed by  $\vec{P}_B$  and  $\vec{P}_T$ , the momentum vectors of the colliding hadrons  $B$  and  $T$ . The  $\hat{x}$  and  $\hat{z}$  axes of the C-S frame both lie in the hadron plane with  $\hat{z}$  axis bisecting the  $\vec{P}_B$  and  $-\vec{P}_T$  vectors. The quark ( $q$ ) and antiquark ( $\bar{q}$ ) annihilate collinearly with equal momenta to form the  $Z$  boson, while the quark momentum vector  $\hat{z}'$  and the  $\hat{z}$  axis form the quark plane. The polar and azimuthal angles of  $\hat{z}'$  in the Collins-Soper frame are  $\theta_1$  and  $\phi_1$ . The  $l^-$  and  $l^+$  are emitted back-to-back with  $\theta$  and  $\phi$  specifying the polar and azimuthal angles of  $l^-$ .

where  $Q$  is the mass of the  $Z$  boson. Equation (2) shows that  $\beta$  vanishes at  $q_T = 0$ , as  $\vec{P}_B$  and  $\vec{P}_T$  are collinear at this limit. For non-zero  $q_T$ ,  $\beta$  increases with  $q_T$ , approaching  $90^\circ$  for  $q_T \gg Q$ . Fig. 2 also shows the “lepton plane” formed by the momentum vector of  $l^-$  and the  $\hat{z}$  axis. The  $l^-$  and  $l^+$  are emitted back-to-back with equal momenta in the rest frame of  $Z$ .

Viewed from its rest frame, the  $Z$  boson must be formed via the annihilation of a pair of collinear  $q$  and  $\bar{q}$  with equal momenta, as illustrated in Fig. 2. We define the momentum unit vector of  $q$  as  $\hat{z}'$ , and the “quark plane” is formed by the  $\hat{z}'$  and  $\hat{z}$  axes. The polar and azimuthal angles of the  $\hat{z}'$  axis are denoted as  $\theta_1$  and  $\phi_1$ , respectively. It is important to note that the  $l^-$  angular distribution must be azimuthally symmetric with respect to the  $\hat{z}'$ , namely,

$$\frac{d\sigma}{d\Omega} \propto 1 + a \cos \theta_0 + \cos^2 \theta_0, \quad (3)$$

where  $\theta_0$  is the angle between the  $l^-$  momentum vector and the  $\hat{z}'$  axis (see Fig. 2), and  $a$  is the forward-backward asymmetry originating from the parity-violating coupling to the  $Z$  boson. Equation (3) shows that the lepton angular distribution has a very simple form when measured with respect to the  $q\bar{q}$  axis.

As  $\theta_0$  is, in general, not an experimental observable, the cross section must be expressed in terms of the observables  $\theta$  and  $\phi$ . This can be accomplished by using the relation

$$\cos \theta_0 = \cos \theta \cos \theta_1 + \sin \theta \sin \theta_1 \cos(\phi - \phi_1). \quad (4)$$

Substituting Eq. (4) into Eq. (3), we obtain the following expression:

$$\begin{aligned} \frac{d\sigma}{d\Omega} \propto & (1 + \cos^2 \theta) + \frac{\sin^2 \theta_1}{2} (1 - 3 \cos^2 \theta) \\ & + \left(\frac{1}{2} \sin 2\theta_1 \cos \phi_1\right) \sin 2\theta \cos \phi \\ & + \left(\frac{1}{2} \sin^2 \theta_1 \cos 2\phi_1\right) \sin^2 \theta \cos 2\phi \end{aligned}$$

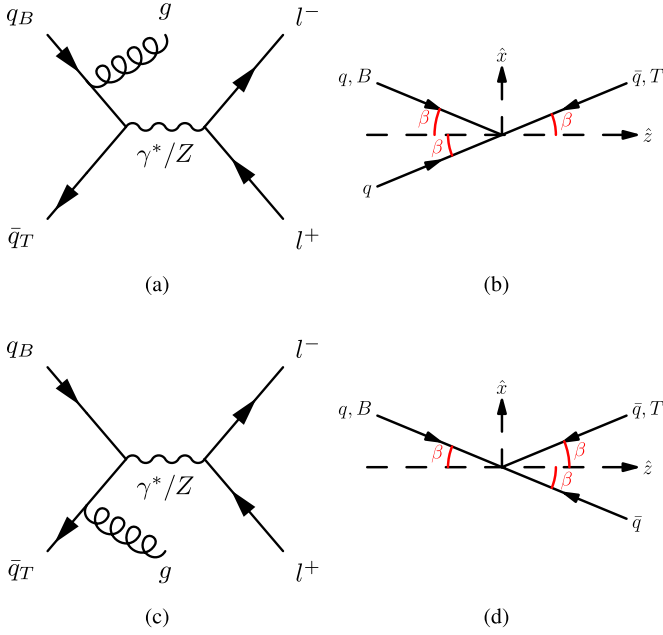


**Fig. 3.** (a) Feynman diagram for  $q\bar{q}$  annihilation where a gluon is emitted from a quark in the hadron  $B$ . (b) Momentum direction for  $q$  and  $\bar{q}$  in the C-S frame before and after gluon emission. Initially, the  $q$  and  $\bar{q}$  are collinear with the hadron  $B$  and  $T$ , respectively. After gluon emission,  $q$  and  $\bar{q}$  become collinear. Note that the  $q$  and  $\bar{q}$  always make an angle  $\beta$  with respect to the  $\hat{z}$  axis in the C-S frame. (c) Feynman diagram for the case where a gluon is emitted from an antiquark in the hadron  $T$ . (d) Momentum direction for  $q$  and  $\bar{q}$  in the C-S frame before and after gluon emission for diagram (c). Again,  $q$  and  $\bar{q}$  become collinear after gluon emission.

$$\begin{aligned}
 &+ (a \sin \theta_1 \cos \phi_1) \sin \theta \cos \phi + (a \cos \theta_1) \cos \theta \\
 &+ \left(\frac{1}{2} \sin^2 \theta_1 \sin 2\phi_1\right) \sin^2 \theta \sin 2\phi \\
 &+ \left(\frac{1}{2} \sin 2\theta_1 \sin \phi_1\right) \sin 2\theta \sin \phi \\
 &+ (a \sin \theta_1 \sin \phi_1) \sin \theta \sin \phi, \tag{5}
 \end{aligned}$$

which is of the same form as Eq. (1). A comparison between Eq. (1) and Eq. (5) shows that  $A_i$  can be expressed in terms of the three quantities,  $\theta_1$ ,  $\phi_1$  and  $a$ , as follows:

$$\begin{aligned}
 A_0 &= \langle \sin^2 \theta_1 \rangle & A_1 &= \frac{1}{2} \langle \sin 2\theta_1 \cos \phi_1 \rangle \\
 A_2 &= \langle \sin^2 \theta_1 \cos 2\phi_1 \rangle & A_3 &= \langle a \sin \theta_1 \cos \phi_1 \rangle \\
 A_4 &= \langle a \cos \theta_1 \rangle & A_5 &= \frac{1}{2} \langle \sin^2 \theta_1 \sin 2\phi_1 \rangle \\
 A_6 &= \frac{1}{2} \langle \sin 2\theta_1 \sin \phi_1 \rangle & A_7 &= \langle a \sin \theta_1 \sin \phi_1 \rangle. \tag{6}
 \end{aligned}$$

Equation (6) is a generalization of an earlier work [12] which considered the special case of  $\phi_1 = 0$  and  $a = 0$ . The  $\langle \dots \rangle$  in Eq. (6) is a reminder that the measured values of  $A_i$  are averaged over the events.

As shown in Eq. (6), the  $q_T$  and  $y$  dependencies of the angular distribution coefficients,  $A_i$ , are entirely governed by the  $q_T$  and  $y$  dependencies of  $\theta_1$ ,  $\phi_1$  and  $a$ . We now consider the quantities  $\theta_1$  and  $\phi_1$ . At the leading-order ( $\alpha_s^0$ ), the quark axis,  $\hat{z}'$ , is collinear with the beam axis. Hence, the result  $\theta_1 = 0$  (or  $\theta_1 = \pi$ ) is obtained, and Eq. (6) shows that all  $A_i$  except  $A_4$  vanish.

At the next-to-leading order (NLO),  $\alpha_s$ , a hard gluon or quark (antiquark) is emitted so that  $Z$  acquires nonzero  $q_T$ . Fig. 3(a) shows the Feynman diagram for the  $q\bar{q}$  annihilation process in which a gluon is emitted from the quark in hadron  $B$ . Fig. 3(b)

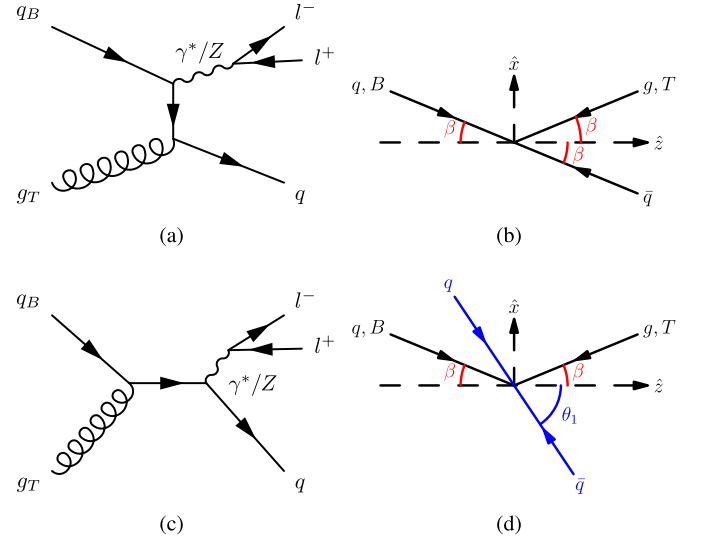


**Fig. 4.** (a) Feynman diagram for  $qg$  Compton process where a quark from hadron  $B$  annihilates with an antiquark from the splitting of a gluon in hadron  $T$ . (b) Momentum direction of  $q$ ,  $\bar{q}$  and  $g$  in the C-S frame before and after gluon splitting. (c) Feynman diagram for  $qg$  fusing into a quark which then emits a  $Z$ . (d) Momentum direction of  $q$ ,  $\bar{q}$  and  $g$  before and after the  $qg$  fusion.

shows that, initially, the  $q$  and  $\bar{q}$  are moving collinearly with the hadron  $B$  and  $T$ , respectively, making an angle  $\beta$  with respect to the  $\hat{z}$  axis. After the gluon emission, the momentum vector of the  $q$  is modified such that it is now opposite to  $\bar{q}$ 's momentum vector in the rest frame of  $Z$ . Since  $\bar{q}$  and hadron  $T$  have the same momentum direction, the  $\hat{z}'$  axis is along the direction of  $-\vec{p}_T$ . From Fig. 2, it is evident that  $\theta_1 = \beta$  and  $\phi_1 = 0$  in this case. Similarly, for the case of Fig. 3(c), where a gluon is emitted from an antiquark in the hadron  $T$ , one obtains  $\theta_1 = \beta$  and  $\phi_1 = \pi$ , as illustrated in Fig. 3(d). Analogous results can be found when the roles of beam and target are interchanged. Given  $\theta_1 = \beta$  (or  $\theta_1 = \pi - \beta$ ) and  $\tan \beta = q_T/Q$  in the Collins-Soper frame, Eq. (6) gives the following result for the NLO  $q\bar{q}$  annihilation processes:

$$A_0 = \sin^2 \theta_1 = q_T^2 / (Q^2 + q_T^2). \tag{7}$$

Since  $\phi_1 = 0$  or  $\pi$ , Eq. (6) shows that the Lam-Tung relation,  $A_0 = A_2$ , is satisfied in this case.

We next consider the Compton process at NLO. Unlike the cases for the  $q\bar{q}$  initial state shown in Fig. 3 where a hard gluon is emitted, a hard quark or antiquark will now accompany the  $Z$  in the final state. Fig. 4(a) shows the diagram in which a gluon from hadron  $T$  splits into a  $q\bar{q}$  pair and the quark from hadron  $B$  annihilates with the antiquark into a  $Z$  boson. Since the momentum vector of the quark in hadron  $B$  is unchanged,  $\theta_1 = \beta$  and  $\phi_1 = \pi$ , as shown in Fig. 4(b). This result is identical to that for the  $q\bar{q}$  initial state shown in Fig. 3(d). Analogous results with  $\theta_1 = \beta$  and  $\phi_1 = 0$  are obtained when gluon is emitted from the beam hadron, or when an antiquark replaces the quark in the initial state. However, a different situation arises, as shown in Fig. 4(c), where the quark and gluon fuse into a quark, which then emits a  $Z$ . As indicated in Fig. 4(d),  $\theta_1$  must satisfy  $\beta \leq \theta_1 \leq \pi - \beta$ , since the momenta of the initial quark and gluon combine vectorially, resulting in a  $\theta_1$  within these two limits. Therefore, the Compton processes would lead to a  $\theta_1$  larger than  $\beta$ , with the exact value governed by the relative weight of these two processes. It was shown by Thews [13] that, to a very good approximation,  $A_0$  for the  $qg$  Compton processes at order  $\alpha_s$  can be given as

$$A_0 = 5q_T^2 / (Q^2 + 5q_T^2). \quad (8)$$

Since  $\phi_1 = 0$  or  $\pi$ , the Lam-Tung relation,  $A_0 = A_2$ , is again satisfied for the Compton process at NLO.

The dotted and dashed curves in Fig. 1(a) correspond to calculations using Eqs. (7) and (8) for the  $q\bar{q}$  annihilation and the  $qg$  Compton processes, respectively. As the  $q\bar{q}$  and  $qg$  processes contribute to the  $pp \rightarrow ZX$  reaction incoherently, the observed  $q_T$  dependence of  $A_0$  reflects the combined effect of these two contributions. A best-fit to the CMS  $A_0$  data gives a mixture of  $58.5 \pm 1.6\%$   $qg$  and  $41.5 \pm 1.6\%$   $q\bar{q}$  processes. The solid curve in Fig. 1(a) shows that the data at both rapidity regions can be well described by this mixture of the  $qg$  and  $q\bar{q}$  processes. For  $pp$  collisions at the LHC, the  $qg$  process is expected to be more important than the  $q\bar{q}$  process, in agreement with the best-fit result. While the amount of  $qg$  and  $q\bar{q}$  mixture can in principle depend on the rapidity,  $y$ , the CMS data indicate a very weak, if any,  $y$  dependence. The good description of  $A_0$  shown in Fig. 1(a) also suggests that higher-order QCD processes do not affect the values of  $\theta_1$  significantly.

We next consider the CMS data on the  $A_2$  coefficient. As shown in Eq. (6),  $A_2$  depends not only on  $\theta_1$ , but also on  $\phi_1$ . In leading order  $\alpha_s$  where only a single undetected parton is present in the final state, the  $\hat{z}'$  axis must lie in the hadron plane, implying  $\phi_1 = 0$  and the Lam-Tung relation is satisfied. We first compare the CMS data, shown in Fig. 1(b), with the calculation for  $A_0 = A_2$ . The dashed curve uses the same mixture of 58.5%  $qg$  and 41.5%  $q\bar{q}$  components as obtained from the  $A_0$  data. The  $A_2$  data are at a variance with this calculation, suggesting the presence of higher-order QCD processes leading to a non-zero value of  $\phi_1$  (see Eq. (6)). We then performed a fit to the  $A_2$  data allowing  $A_2/A_0$  to be different from 1, caused by a non-zero value of  $\phi_1$ . The best-fit value is  $A_2/A_0 = 0.77 \pm 0.02$ . The solid curve in Fig. 1(b) corresponds to the best fit to the data. The non-zero value of  $\phi_1$  implies that the Lam-Tung relation,  $A_0 = A_2$ , is violated. This violation is shown explicitly in Fig. 1(c). The solid curve obtained with  $A_2/A_0 = 0.77$  describes the observed violation of the Lam-Tung relation well.

The violation of the Lam-Tung relation reflects the non-coplanarity between the quark plane and the hadron plane (i.e.,  $\phi_1 \neq 0$ ). This can be caused by higher-order QCD processes, where multiple partons, in addition to the detected  $Z$ , are present in the final state.

The angular distribution results reported by the CMS Collaboration correspond to inclusive  $Z$  boson production. Based on the analysis presented above, we expect that interesting new results would be obtained if the data were analyzed according to the multiplicity and types of jets accompanying the  $Z$ -boson. In particular, we have the following predictions:

a) For  $Z$  plus single-jet events, Fig. 1(a) shows that the  $q_T$  dependence for  $A_0$  is very different between the  $q\bar{q}$  annihilation process and the  $qg$  Compton process. Since the  $q\bar{q}(qg)$  process contains an associated high- $p_T$  gluon (quark) jet at the  $\alpha_s$  level, as shown in Figs. 3 and 4, one could utilize the existing algorithms for quark (gluon) jet identification to separate the  $q\bar{q}$  annihilation events from the  $qg$  Compton events. Therefore, we predict that the  $Z$  plus single quark-jet events would give a distinctly different  $A_0$  from that of  $Z$  plus single gluon-jet events. These  $Z$  plus single jet  $A_0$  data can also provide a powerful experimental tool to test various algorithms for discriminating a quark jet from a gluon jet [14–16].

b) As all  $A_i$  coefficients depend on the values of  $\theta_1$  (see Eq. (6)), we expect that the  $q_T$  dependence of all  $A_i$ , not just  $A_0$ , would be different for the  $q\bar{q}$  annihilation and the  $qg$  Compton events. This prediction can be readily tested from the existing  $Z$  production data. Furthermore, these  $A_i$  angular coefficients would provide

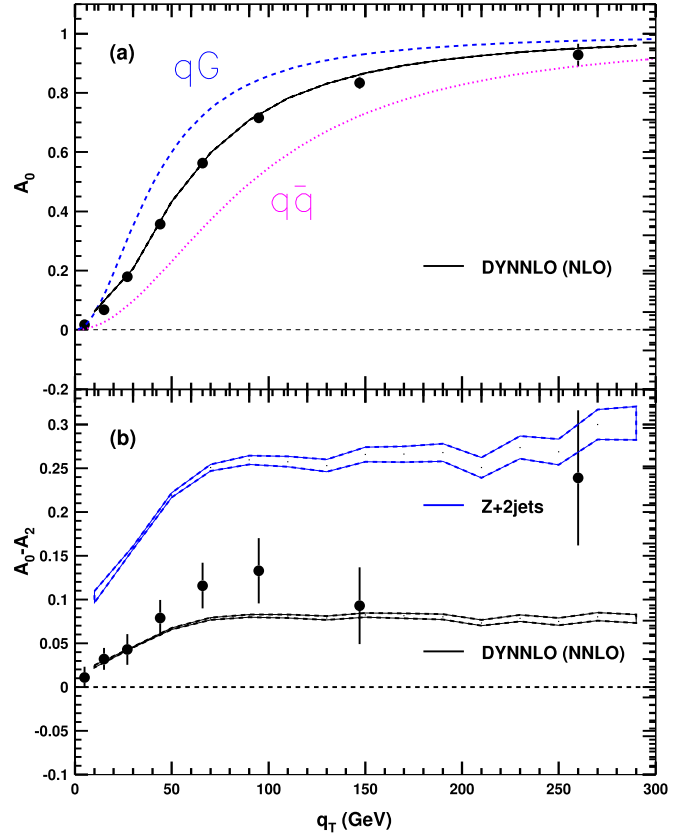


Fig. 5. Comparison between the CMS data on  $A_0$  and  $A_0 - A_2$  with perturbative QCD calculations. Curves correspond to calculations described in the text.

additional experimental tools for testing the algorithms for discriminating quark from gluon jets.

c) As discussed above, the Lam-Tung relation is expected to be valid for  $Z$  plus single-jet events. Hence, the angular distributions data for these single jet events are predicted to satisfy  $A_0 = A_2$  at all values of rapidities and  $q_T$ . This remains to be tested with the high statistics  $Z$  production data from the LHC.

d) For the  $Z$  plus multi-jet data, the Lam-Tung relation is expected to be violated at a higher level than that of the inclusive  $Z$  production data. Removal of the  $Z$  plus single-jet events, which must satisfy the Lam-Tung relation, would enhance the violation of the Lam-Tung relation. Again, this can be tested with existing LHC data [17,18].

To illustrate the points discussed above, we have carried out perturbative QCD calculations using the code DYN NLO [19,20]. The parton distribution functions used in the NLO and NNLO calculations are the CT14nlo and CT14nnlo sets. Fig. 5(a) shows the comparison between the CMS  $A_0$  data at  $|y| < 1.0$  and the perturbative QCD calculation at the order  $\alpha_s$ . The large difference in  $A_0$  for the  $q\bar{q}$  and  $qg$  processes is consistent with the results shown in Fig. 1(a) obtained with the geometric model. This lends support to the expectation that one can use the  $Z$  plus single-jet events to test the various jet identification algorithms.

Fig. 5(b) compares the DYN NLO calculations with the CMS  $A_0 - A_2$  data. The black band corresponds to the NNLO calculation including contributions from single jet and two jets. The blue band singles out the contributions to  $A_0 - A_2$  from  $Z$  plus 2 jets only, showing that the violation of the Lam-Tung relation is indeed amplified for the multi-jet events. This can be readily tested with the data collected at the LHC.

In summary, we have presented an intuitive interpretation for the lepton angular distribution coefficients for  $Z$  boson production

in hadron collision. We first derive the general expression (Eq. (5)) for the lepton polar and azimuthal angular distribution in the  $Z$  boson rest frame, starting from the azimuthally symmetric lepton angular distribution (Eq. (3)) with respect to the quark-antiquark axis. We show that the various angular distribution coefficients are governed by three quantities,  $\theta_1$ ,  $\phi_1$  and  $a$  (Eq. (6)). The  $q_T$  dependence of  $A_0$  is found to be very well described using the leading-order results for  $\theta_1$ . It also allows a determination of the relative fractions of these two processes. This result is noteworthy, as it shows that a measurement of the angular distribution coefficient  $A_0$  alone could lead to important information on the dynamics of the production mechanism, namely, the relative contribution of the  $q\bar{q}$  annihilation and the  $qG$  Compton processes.

The CMS data clearly show that the Lam-Tung relation,  $A_0 = A_2$ , is violated. The origin of this violation is attributed in our approach to the deviation of  $\phi_1$  from zero, indicating the non-coplanarity between the hadron and quark planes. This non-coplanarity is caused by higher-order QCD processes. We show that the amount of non-coplanarity can be deduced from the  $A_0 - A_2$  data directly.

We discuss how the measurement of  $A_0$  and  $A_2$  coefficients in  $Z$  plus single-jet or multi-jet events would provide valuable insight on the origin of the violation of the Lam-Tung relation. We also show that the  $A_0$  coefficient in  $Z$  plus single-jet events would be a powerful tool for testing various algorithms which discriminate quark jets from gluon jets.

### Acknowledgements

This work was supported in part by the U.S. National Science Foundation and the Ministry of Science and Technology of Tai-

wan. It was also supported in part by the U.S. Department of Energy, Office of Science, Office of Nuclear Physics under contract DE-AC05-06OR23177.

### References

- [1] E. Mirkes, J. Ohnemus, Phys. Rev. D 50 (1994) 5692.
- [2] E.L. Berger, L.E. Gordon, M. Klasen, Phys. Rev. D 58 (1998) 074012.
- [3] CDF Collaboration, T. Aaltonen, et al., Phys. Rev. Lett. 106 (2011) 241801.
- [4] CMS Collaboration, V. Khachatryan, et al., Phys. Lett. B 749 (2015) 187.
- [5] ATLAS Collaboration, G. Aad, et al., J. High Energy Phys. 08 (2016) 159.
- [6] C.S. Lam, W.K. Tung, Phys. Rev. D 18 (1978) 2447.
- [7] C.G. Callan, D.J. Gross, Phys. Rev. Lett. 22 (1969) 156.
- [8] J.C. Peng, W.C. Chang, R.E. McClellan, O. Teryaev, Phys. Lett. B 758 (2016) 384.
- [9] W.C. Chang, R.E. McClellan, J.C. Peng, O. Teryaev, Phys. Rev. D 96 (2017) 054020.
- [10] S.D. Drell, T.M. Yan, Phys. Rev. Lett. 25 (1970) 316, Ann. Phys. (NY) 66 (1971) 578.
- [11] J.C. Collins, D.E. Soper, Phys. Rev. D 16 (1977) 2219.
- [12] O.V. Teryaev, in: Proceedings of XI Advanced Research Workshop on High Energy Spin Physics, Dubna, 2005, pp. 171–175.
- [13] R.L. Thews, Phys. Rev. Lett. 43 (1979) 987.
- [14] ATLAS Collaboration, G. Aad, et al., Eur. Phys. J. C 74 (2014) 3023.
- [15] CMS Collaboration, Technical Report No. CMS-DP-2016-070, 2016.
- [16] E.M. Metodiev, J. Thaler, Phys. Rev. Lett. 120 (2018) 241602.
- [17] ATLAS Collaboration, M. Aaboud, et al., Eur. Phys. J. C 77 (2017) 361.
- [18] CMS Collaboration, A.M. Sirunyan, et al., Eur. Phys. J. C 78 (2018) 962.
- [19] S. Catani, M. Grazzini, Phys. Rev. Lett. 98 (2007) 222002.
- [20] S. Catani, et al., Phys. Rev. Lett. 103 (2009) 082001.